

Influence of soot aerosol properties on the counting efficiency of ~~PN-PTI~~ instruments used for the periodic technical inspection of diesel vehicles

Tobias Hammer¹, Diana Roos¹, Barouch Giechaskiel², Anastasios Melas², Konstantina Vasilatou¹

¹Department of Chemistry, Federal Institute of Metrology METAS, Bern-Wabern, 3003, Switzerland

² European Commission, Joint Research Centre (JRC), 21027 Ispra, Italy

Correspondence to: Konstantina Vasilatou (konstantina.vasilatou@metas.ch)

Abstract. In this work, we investigated the influence of different types of soot aerosol on the counting efficiency (CE) of instruments employed for the periodic technical inspection (PTI) of diesel vehicles. Such instruments report particle number (PN) concentration. Combustion aerosols were generated by a prototype bigCAST, a miniCAST 5201 BC, a miniCAST 6204 C and a miniature inverted soot generator (MISG). For comparison purposes, diesel soot was generated by a Euro 5b diesel test vehicle with by-passed diesel particulate filter (DPF). The size-dependent counting efficiency profile of six PN-PTI instruments was determined with each one of the aforementioned test aerosols. The results showed that the type of soot aerosol affected the response of the PN-PTI sensors in an individualised manner. Consequently, it was difficult to identify trends and draw conclusive results about which laboratory-generated soot is the best proxy for diesel soot. Deviations in the counting efficiency remained typically within 0.25 units when using laboratory-generated soot compared to Euro 5b diesel soot of similar mobility diameter (~50-60 nm). Soot with a mobility diameter of ~100 nm generated by the MISG, the lowest size we could achieve, resulted in most cases in similar counting efficiencies as that generated by the different CAST generators at the same particle size, showing that MISG may be a satisfactory - and affordable - option for PN-PTI verification; however, further optimization will be needed for low-cost soot generators to comply with European PN-PTI verification requirements.

1 Introduction

Soot particles emitted by transport sources can have adverse health effects (Kheirbek et al., 2016; US-EPA, 2019; WHO, 2021). To reduce particulate emissions, new procedures for the periodic technical inspection (PTI) of diesel vehicles based on the measurement of particle number (PN) concentration have recently been established in Switzerland, Germany, the Netherlands and Belgium, while other countries might follow in due time (EU, 2023; Vasilatou et al., 2022). Portable instruments known as PN-PTI counters are used for measuring particle number concentration (PNC) directly in the tailpipe of diesel vehicles equipped with a diesel particle filter (DPF) (Kesselmeier and Staudt, 1999; Melas et al., 2021, 2022, 2023). When the DPF is intact, the emitted PNC is low (typically up to a few thousand particles per cm³), whereas if the DPF is defect or tampered, PNC increases to several hundred thousand particles per cm³ (Botero et al., 2023; Burtscher et al., 2019; Giechaskiel et al., 2022). In terms of particle mass concentration, a functioning DPF can reduce particulate emissions by up to a factor of 150 (Ligterink, 2018) while in terms of particle number concentration a solid particle number trapping efficiency of higher than 99 % has been reported in the literature (Frank, Adam et al., 2020). It has been shown that a small

37 fraction (about 10 %) of vehicles with defective DPF is responsible for up to 80-90 % of the total fleet emissions
38 (Burtscher et al., 2019; Kurniawan and Schmidt-Ott, 2006). The goal of PN-PTI procedures is to identify diesel
39 vehicles with compromised DPFs, thus ensuring that vehicles in operation maintain their performance as
40 guaranteed by type-approval, without excessive degradation, throughout their lifetime (EU, 2023).

41 Although the concept of PN-PTI is simple, its implementation in practice is not as straightforward. PTI procedures
42 are not fully harmonised and, as a result, the limit values for the emitted PNC, the technical specifications of the
43 PN-PTI counters and the test protocol for type-examination and verification are defined at a national level (Anon,
44 n.d.; AU-Richtlinie, n.d.; PTB, 2021; UVEK, 2023; VAMV, 2018; Vasilatou et al., 2022, 2023). Differences in
45 national legislations might lead to contradicting results, e.g. the same diesel vehicle might pass the PTI check in
46 one country but fail in another one. To ensure fair implementation of regulations across Europe and avoid
47 unnecessary costs which may occur for vehicle owners after a False Fail, the various PTI procedures must be
48 compared and the differences elucidated.

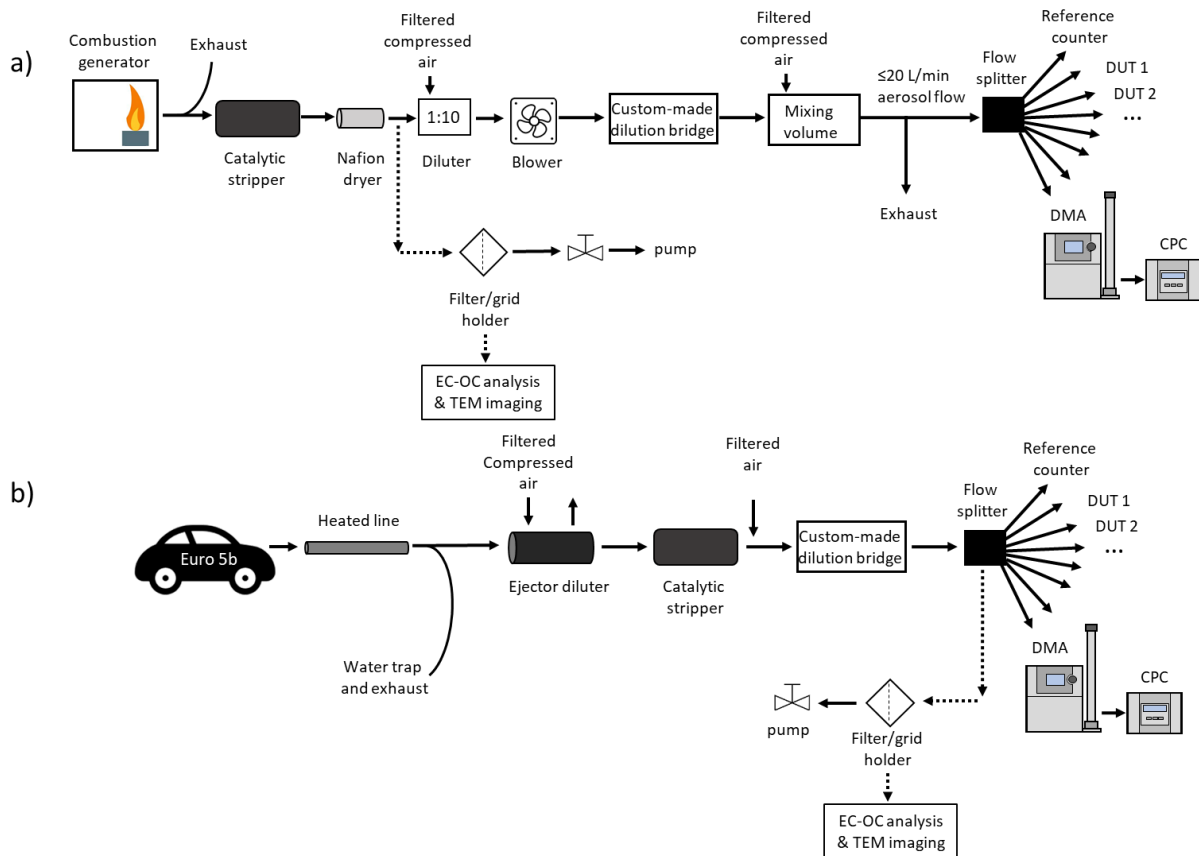
49 PN-PTI instruments go through a type-examination procedure which may differ in each country. Among several
50 tests, type-examination includes a counting efficiency and a linearity check typically performed with combustion
51 aerosols. During their lifetime, PN-PTI instruments are checked for their linearity with polydisperse particles
52 (typically with a GMD of 70 ± 20 nm). In our previous study (Vasilatou et al., 2023), we showed that the choice
53 of test aerosol during type-examination or verification of PN-PTI instruments significantly affects the performance
54 of instruments based on diffusion charging (DC). When sodium chloride (NaCl) or carbonaceous particles from
55 spark-discharge generators were used as test aerosols, the counting efficiency of the DC-based instruments
56 changed by up to a factor of two compared to that exhibited with diesel soot. The experiments clearly showed that
57 soot from laboratory-based combustion generators was the best proxy for soot emitted by diesel engines, however,
58 potential differences between the different combustion generators available on the market were not investigated.
59 In this study, we challenged six different DC-based PN-PTI instruments with polydisperse soot particles produced
60 by three different CAST generators (Jing AG, Switzerland), the miniature inverted soot generator (MISG,
61 Argonaut Scientific, Canada) and a Euro 5b diesel vehicle. The geometric mean diameter of the test aerosol was
62 in the range used for linearity checks of PN-PTI instruments as well as in typical size range emitted by diesel
63 engines. The scope of our study was to investigate possible differences that may arise when using different
64 combustion aerosol generators during the type-examination and verification of PN-PTI instruments as well as to
65 correlate with diesel engine emitted soot. We focused on DC-based instruments because we expect a larger impact
66 of the aerosol properties on their response compared to CPC-based ones (Vasilatou et al., 2023). The size-
67 dependent counting efficiency of the PN-PTI instruments was determined by using a condensation particle counter
68 (NPET 3795, TSI Inc., USA) as a reference instrument. We discuss the results in the context of the different
69 national legislations and make recommendations for the harmonisation of the various calibration and verification
70 procedures in the laboratory.

71 **2 Materials and methods**

72 During the first measurement campaign at METAS, the following laboratory-based diffusion or premixed flame
73 generators were used to produce test aerosols: a prototype bigCAST, a miniCAST 5201 BC (Ess et al., 2021b; Ess
74 and Vasilatou, 2019), a miniCAST 6204 C and the miniature inverted soot generator (MISG) (Giechaskiel and
75 Melas, 2022; Kazemimanesh et al., 2019; Moallemi et al., 2019; Senaratne et al., 2023). By varying the operation

76 points of the CAST generators, polydisperse aerosols with a geometric mean mobility diameter (GMD_{mob}) ranging
77 from 50 nm to 100 nm were generated, as summarised in Fig. S1. In the case of the MISG, particles with a GMD_{mob}
78 down to 100 nm were produced in a repeatable and stable manner using a mixture of dimethyl ether and propane
79 (Senaratne et al., 2023). This is in agreement with another study, where the modal diameter varied between 95 and
80 158 nm (Bischof et al., 2020).

81 The counting efficiency profiles (CE) of six DC-based PN-PTI counters, namely the AEM (TEN, the Netherlands),
82 HEPaC (developed by the University of Applied Sciences Northwestern Switzerland and distributed by Naneos
83 GmbH, Switzerland), DiTEST (AVL DiTEST, Austria), CAP3070 (Capelec, France), DX280 (Continental
84 Aftermarket & Services GmbH, Germany) and AIP PDC KG4 (referred to as Knestel hereafter, KNESTEL
85 Technologie & Elektronik GmbH, Germany) were determined experimentally. The HEPaC, DiTEST, CAP3070
86 and DX280 had been type-approved at METAS according to the Swiss regulations (VAMV, 2018) whereas the
87 Knestel instrument had been type-approved according to the German regulation (AU-Richtlinie, n.d.). The
88 experimental setup at METAS is depicted in Fig. 1a. Soot produced by CAST-burners or the MISG was passed
89 through a catalytic stripper (Catalytic Instruments GmbH, Germany), a Nafion dryer (MD-700-12S-1, PERMA
90 PURE, U.S.A.), a VKL 10 diluter (Palas GmbH, Germany) and a custom-made dilution bridge, and was mixed
91 and diluted with filtered air in a 27-ml-volume chamber. To deliver the aerosol into the mixing volume, a blower
92 (Micronel AG, Switzerland) was used. The aerosol was split with a custom-made 8-port flow splitter and delivered
93 simultaneously to the devices under test (DUT, in this case PN-PTI instrument) and the reference particle counter
94 (NPET 3795, TSI Inc., USA). The splitter bias was determined according to the procedure specified in the ISO
95 27891 standard and was found to be within 1 % for particles with a GMD_{mob} equal to or larger than 23 nm. In
96 addition, the length of the tubes from the flow splitter to the devices was adapted to the respective flow rate to
97 ensure equal diffusion losses. The NPET was selected as reference instrument for two reasons; i) it could be used
98 in field measurements as it included a dilution system, a volatile particle remover and a particle counter, ii) during
99 type examination portable PN-PTI instruments are typically used as reference. NPET had been calibrated in a
100 traceable manner according to the ISO 27891 standard, and showed a CE of 0.77 ± 0.02 , 0.77 ± 0.01 , 0.80 ± 0.01
101 and 0.79 ± 0.02 at a GMD_{mob} of 50 nm, 70 nm, 80 nm and 100 nm, respectively and this counting efficiency was
102 taken into account during data analysis (i.e. a calibration factor of 1.28 was applied to the concentrations reported
103 by the NPET).



104
105
106
107
108

Figure 1: a) Experimental setup for the verification of PN-PTI instruments in the laboratory. Four different combustion generators were used (see text for more details). DUT stands for device under test. Dashed arrows designate measurements which were performed separately, i.e. not in parallel with PN-PTI verification. b) Experimental setup as used for field measurements at JRC.

109
110
111
112
113
114
115
116
117
118
119
120
121
122
123
124
125
126

Mobility size distributions were recorded simultaneously by a scanning mobility particle sizer (^{85}Kr source 3077A, DMA 3081 and butanol CPC 3776, TSI Inc., USA). To analyse the morphology of the soot particles, particles were sampled for 5 s with a flow rate of 1.2 L/min downstream the Nafion dryer, collected on copper-coated TEM (transmission electron microscopy) grids placed in a mini particle sampler (MPS, Ecomeasure, France) and analysed with a Spirit Transmission EM (Tecnai, FEI Company, USA). Soot particles were also sampled on QR-100 Advantec filters (Toyo Roshi Kaisha, Ltd. Japan, preheated at 500 °C for > 1 h) for durations of 15 – 30 min. Elemental carbon (EC) to total carbon (TC) mass fractions were measured with an OC/EC Model 5L analyser (Sunset Laboratory Inc., NL) by applying an extended EUSAAR-2 protocol (Ess et al., 2021b, 2021a).

In a second measurement campaign at JRC, the HEPaC, DiTEST, CAP3070 and DX280 counters were challenged with real diesel engine exhaust from a Euro 5b vehicle. Fig. 1b depicts the experimental setup at JRC. Soot from engine exhaust was passed through a water trap, a heated line (150 °C) to avoid water condensation, an ejector dilutor (DI-1000, Dekati, Finland), a catalytic stripper (Catalytic Instruments GmbH, Germany) to remove (semi)volatile organic matter, and was diluted to the required concentrations with a custom-made dilution bridge. It has been shown that the ejector dilutor does not affect the particle size distribution (Giechaskiel et al., 2009). PNC was recorded for several minutes, which allowed identifying long-time trends or drifts of the reported PNC. In addition, PNCs were averaged over a period of 1 min, thus the duration was similar to the duration of real PN-PTI tests which varies from 15 to 90 s. Mobility size distributions were measured by an SMPS, consisting of an ^{85}Kr source (3077A, TSI Inc., U.S.A.; purchased in 2021), a DMA 3081 and a CPC 3010 (TSI Inc., USA).

127 A Euro 5b vehicle with by-passed DPF was tested as real source of diesel soot. The vehicle generated size
 128 distributions with a GMD_{mob} of $56.4 \text{ nm} \pm 0.7 \text{ nm}$. Diesel particles from the Euro 5b vehicle were collected on
 129 TEM grids [and quartz filters](#) and analysed as described above.

130 The fractal dimension D_f of size-selected soot particles with a nominal GMD_{mob} mobility diameter d_p of 100 nm
 131 was derived via image analysis of high-quality TEM-images using the FracLac feature of ImageJ 1.53e (ImageJ,
 132 National Institutes of Health, USA). In a first step, the greyscale TEM-images were converted into binary images
 133 utilizing the auto-convert function of FracLac. In a second step, the D_f values were determined via the so-called
 134 box counting, averaging 12 rotations of each image. The effective density was determined for the 100 nm setpoints
 135 using an Aerodynamic Aerosol Classifier (AAC, Cambustion, UK) and a DMA (TSI Inc., USA) in tandem as
 136 described in (Tavakoli and Olfert, 2014).

137 3 Results

138 3.1 Aerosol properties

139 Particle number concentration measured by diffusion chargers depends on the average number of charges carried
 140 by each particle (Fierz et al., 2011). Particle size and morphology have been shown to have an effect on the number
 141 of charges carried by the particles and, thus, on the counting efficiency of diffusion charger based PN-PTI
 142 instruments (see (Dhaniyala et al., 2011; Vasilatou et al., 2023) and references therein). Soot particles from
 143 complex structures described by a fractal-like scaling law (Mandelbrot, 1982), and their mobility is influenced by
 144 their morphology (described by the fractal dimension and fractal pre-factor) and the momentum-transfer regime
 145 (Filippov et al., 2000; Melas et al., 2014; Sorensen, 2011). To characterise the soot particles produced by the
 146 different aerosol generators, the following aerosol properties were determined: particle size distribution, EC/TC
 147 ratio, primary particle size and fractal dimension. EC/TC ratio can also have an effect on the morphology of the
 148 soot particles. Soot particles formed in premixed flames (i.e. high EC/TC) exhibit a loose agglomerate structure
 149 where the primary particles are clearly distinguishable from one another, while soot generated in fuel-rich flames
 150 (high OC/TC) has a more compact structure and the primary particles tend to merge with each other (see Fig. 3 in
 151 (Ess et al., 2021b)). [OC stands for organic carbon.](#)

152
 153 The properties of the soot aerosols are summarised in Table 1. Mobility size distributions [and TEM images](#) are
 154 shown in Fig. S1 [and Fig. 2, respectively.](#)

155 **Table 1: Physical properties of the soot aerosols produced by the various combustion generators and the Euro 5b engine.**
 156 [GMD_{mob} and GSD stand for geometric mean mobility diameter and geometric standard deviation. EC and TC denote elemental](#)
 157 [and total carbon. \$d_{pp}\$, \$\rho_{eff}\$ and \$D_f\$ are the primary particle diameter, effective density and fractal dimension of soot particles.](#)

| Soot generator | Setpoint | GMD_{mob} (nm) | GSD (nm) | EC/TC mass fraction (%)* | d_{pp} (nm)** | ρ_{eff} (g/cm ³)*** | $D_f^{\dagger\dagger}$ |
|--------------------|----------|------------------|----------|--------------------------|-----------------|--------------------------------------|---|
| MISG | 100 nm | 103.3 | 1.76 | 86.2 ± 10 | 9.2 ± 2.8 | 0.91 ± 0.02 | 1.71 63 ± 0.03 08 |
| miniCAST 6204 C | 50 nm | 50.7 | 1.43 | 57.2 ± 8.9 | | | |
| | 70 nm | 73.4 | 1.48 | 27.9 ± 4.6 | | | |
| | 80 nm | 80.0 | 1.54 | 77.8 ± 9.0 | | | |

| | | | | | | | |
|---------------------|---------------------|-------|-----------------|-----------------|--|-------------------------|--|
| | 100 nm | 99.5 | 1.69 | 41.9 ± 6.5 | 21.6 ± 2.5 | 0.35 ± 0.04 | 1.54 ₆₄ ± 0.04 ₀₉ |
| miniCAST 5201 BC | 50 nm | 51.1 | 1.60 | 100 ± 18.5 | | | |
| | 70 nm fuel-lean | 75.3 | 1.59 | 94.6 ± 15.6 | | | |
| | 70 nm fuel-rich | 74.2 | 1.69 | 73.7 ± 11.4 | | | |
| | 80 nm | 81.8 | 1.57 | 98.1 ± 15.3 | | | |
| | 100 nm fuel-lean | 99.8 | 1.63 | 97.4 ± 9.6 | $15.8 \pm 3.5^\dagger$ | $\sim 0.4^\dagger$ | 1.58 ₅₅ ± 0.04 ₁₁ |
| | 100 nm fuel-rich | 101.9 | 1.58 | 65.7 ± 10.0 | Primary particles are partly merged [†] | $1.04 \pm 0.16^\dagger$ | 1.71 ₆₅ ± 0.04 ₀₈ |
| bigCAST | 50 nm | 52.5 | 1.57 | 50.9 ± 11.7 | | | |
| | 70 nm | 71.6 | 1.54 | 62.2 ± 13.3 | | | |
| | 80 nm | 81.5 | 1.53 | 81.2 ± 8.8 | | | |
| | 100 nm | 98.9 | 1.60 | 100.0 ± 9.0 | 24.5 ± 1.8 | 0.66 ± 0.04 | 1.66 ₅₇ ± 0.02 ₀₅ |
| Vehicle Euro 5b | | 56.4 | 2.12 ± 0.00 | 83.5 ± 20.5 | 19.7 ± 4.4 | | 1.67 ± 0.03 |

158 * Uncertainties of the EC/TC mass fraction (downstream of the CS) are estimated to be in the range of 10-15 %.

159 Uncertainties due to the split point could not be quantified and were not taken into account.

160 ** Expanded uncertainty ($k=2$, 95 % confidence interval) determined as the twofold standard deviation of d_{pp} , of
161 at least 20 primary particles of various mature soot particles divided by the square route of the number of
162 measurements.

163 *** Expanded uncertainty ($k=2$, 95 % confidence interval) determined as the twofold standard deviation of three
164 measurements.

165 † Taken from (Ess et al., 2021b).

166 †† Expanded uncertainty ($k=2$, 95 % confidence interval) determined as the twofold standard deviation of at least
167 10 measurements.

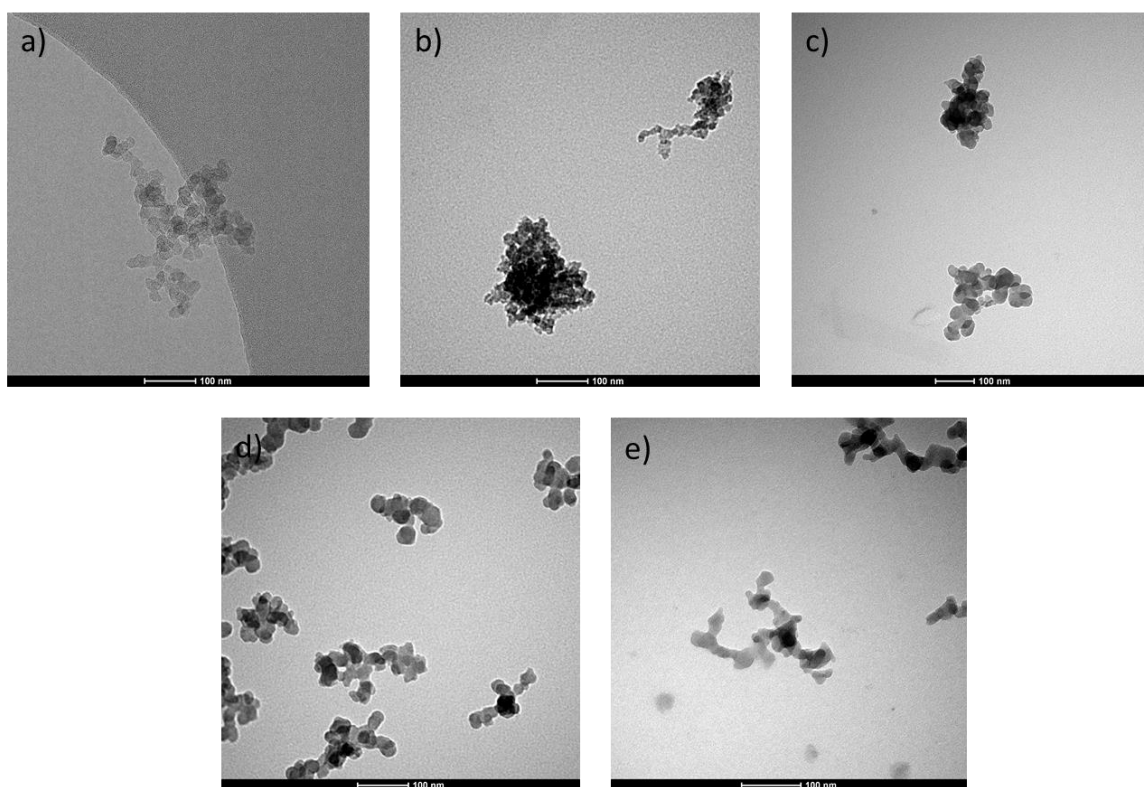
168

169 ~~The fractal dimension D_f of soot particles with a nominal GMD_{nom} of 100 nm was derived via image analysis of~~
170 ~~high-quality TEM images using the Fraclac feature of ImageJ 1.53c (ImageJ, National Institutes of Health, USA).~~
171 ~~In a first step, the greyscale TEM images were converted into binary images utilizing the auto-convert function of~~
172 ~~Fraclac. In a second step, the D_f values were determined via the so-called box counting, averaging 12 rotations of~~
173 ~~each image. The D_f values summarised in Table 1 represent the average values obtained from at least ~~10-20~~~~
174 ~~particles for each type of soot. These values agree well with those reported in previous studies for bare (i.e. freshly~~
175 ~~emitted) soot particles (Pang et al., 2022; Wang et al., 2017).~~

176 ~~The effective density was determined for the 100 nm setpoints using an Aerodynamic Aerosol Classifier (AAC,~~
177 ~~Cambustion, UK) and a DMA (TSI Inc., USA) as described in (Tavakoli and Olfert, 2014). The lowest effective~~

178 density ($0.35 \pm 0.02 \text{ g/cm}^3$) was found for particles generated by the miniCAST 6204 C. Considering that these
 179 particles contain a high amount of OC, this value might seem at first glance to be low, but can be explained by the
 180 highly fractal-like structure of soot (Fig. 2e). In comparison, the miniCAST 5201 BC produced particles with an
 181 effective density of $1.04 \pm 0.08 \text{ g/cm}^3$ when operated under fuel-rich conditions (i.e. high OC mass fraction), which
 182 is in line with the more compact structure as shown in (Ess et al., 2021b). Similarly, the MISG generated particles
 183 with an effective density of $0.91 \pm 0.02 \text{ g/cm}^3$. 100 nm particles generated by the bigCAST exhibited an
 184 intermediate effective density of $0.66 \pm 0.02 \text{ g/cm}^3$. [According to the summary work by Olfert and Rogak, the](#)
 185 [effective density of denuded soot from various sources \(gas turbines, compression ignition engines and laboratory-](#)
 186 [based burners\) lies typically in the range 0.4-0.8 g/cm³ at 100 nm mobility diameter](#) (Olfert and Rogak, 2019).
 187 [Compression-ignition engines tend to produce soot with higher effective densities, while gas-turbine soot tends to](#)
 188 [have lower effective densities](#) (Olfert and Rogak, 2019). ~~The results are in line with the~~ The calculated fractal
 189 dimension of soot particles [lies in the range 1.55 – 1.65 for all generators, in line with the fractal-like morphology](#)
 190 [observed in the TEM images and with previous studies on freshly emitted soot particles from different combustion](#)
 191 [sources](#) (Pang et al., 2023), ~~which increases from 1.54 for soot generated by the miniCAST 6204 C to 1.71 for~~
 192 ~~soot generated by the MISG.~~

193



194
 195 **Figure 2: TEM images of polydisperse soot particles generated by a) the miniCAST 5201 BC (GMD_{mob} of ~100 nm, fuel-**
 196 **lean setpoint); b) the MISG (GMD_{mob} of ~100 nm); c) by the Euro 5b test vehicle (GMD_{mob} of ~55 nm); d) the prototype**
 197 **bigCAST (GMD_{mob} of ~100 nm); and e) by the miniCAST 6204 C (GMD_{mob} of ~100 nm). Further images are compiled**
 198 **in Figs. S2-S5 and in (Ess et al., 2021b).**

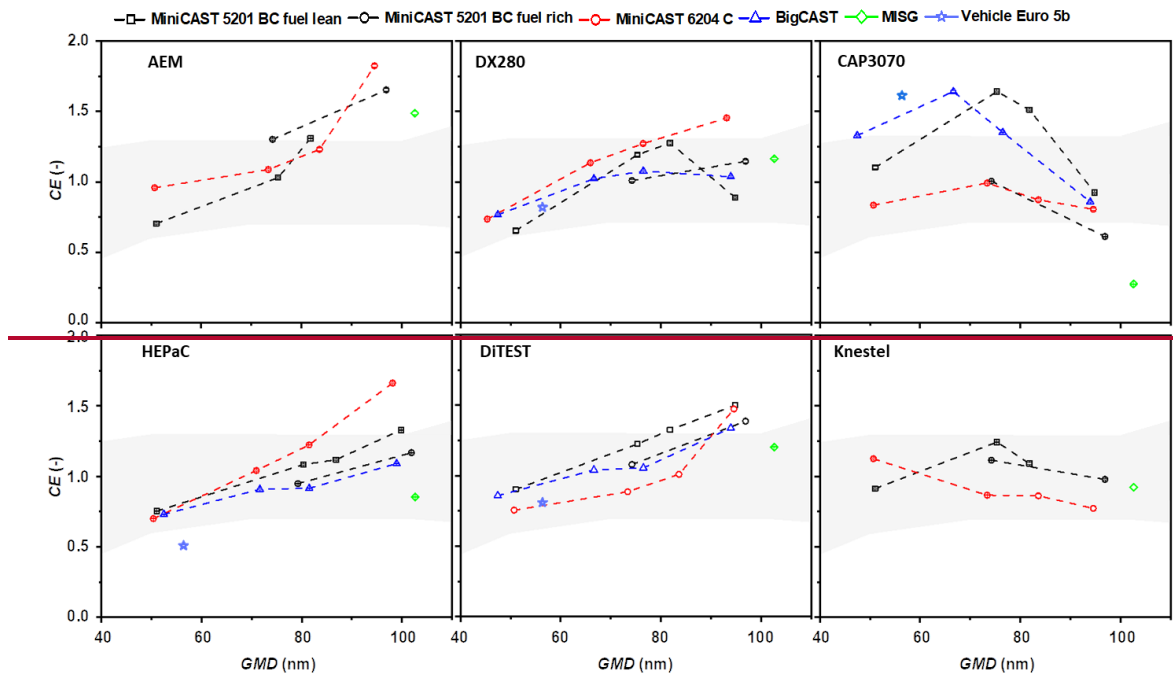
199 Soot particles generated by the bigCAST with a GMD_{mob} of ~ 100 nm consist of primary particles with a diameter
 200 $d_{pp} = 24.5 \text{ nm} \pm 1.8 \text{ nm}$, whereas those from miniCAST 5201 BC (fuel lean setpoint) have an average primary
 201 particle size of $12.3 \text{ nm} \pm 3.7 \text{ nm}$ at a similar GMD_{mob}. Soot generated by the MISG had a much smaller primary
 202 particle size (d_{pp} of $9.2 \text{ nm} \pm 3.8 \text{ nm}$). The TEM images in Figs. 2b and S3 revealed that some particles have a

203 more compact soot structure than what reported by (Kazemimanesh et al., 2019) who used ethylene as fuel. This
204 observation is in line with the relatively high particle effective density (0.91 g/cm^3) and fractal dimension (1.71)
205 reported above.

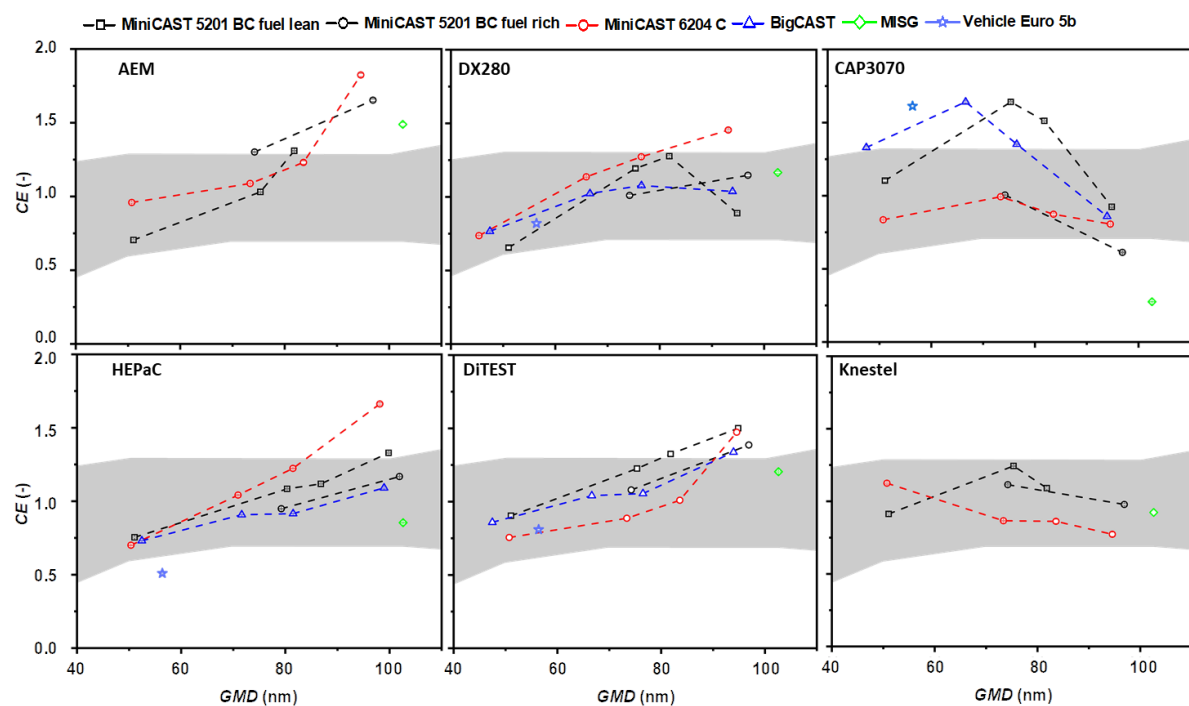
206 3.2 Counting efficiency (CE) profiles of PN-PTI counters

207 The CE profiles of the PN-PTI instruments under test were determined by dividing the reported number
208 concentration by that measured with a reference condensation particle counter (NPET 3795, TSI Inc., USA). The
209 counting efficiency of the reference counter was taken into account during the data analysis.

210 Figure 3 summarises the results obtained with the various laboratory-based combustion generators and the Euro
211 5b diesel vehicle. In general, the CE of PN-PTI instruments increased with increasing GMD_{mob} , in line with
212 previous studies (Melas et al., 2023; Vasilatou et al., 2023). In the case of CAP3070, CE started to decrease at
213 $\text{GMD}_{\text{mob}} \geq 65 \text{ nm}$, most probably due to built-in correction factors. It cannot be ruled out that the measurement
214 principle of the instrument, based on the so-called escaping current principle, plays also a role (Lehtimäki, 1983).
215 In general, for each PN-PTI instrument, the differences in CE when challenged with different soot aerosols of
216 similar particle size were <0.25 at 50 nm and increased with size, but remained typically lower than 0.5. Higher
217 differences were observed for CAP3070 at around 100 nm, probably related to the internal correction factors. This
218 indicates that the exact morphology (e.g. primary particle size, effective density) of the test aerosol had an effect
219 on instrument performance as expected from previous studies (Dhaniyala et al., 2011). The response of each PN-
220 PTI model was, however, individual, making it difficult to draw any general trends. For instance, the CE of the
221 HEPaC was higher when measuring soot particles from the miniCAST 6204 C compared to soot of similar
222 GMD_{mob} from the bigCAST. CAP3070 showed the opposite behaviour. At a GMD_{mob} of $\sim 100 \text{ nm}$, DX280
223 exhibited a higher CE with soot particles generated by the miniCAST 5201 BC under fuel-rich conditions (i.e.
224 lower EC/TC mass fraction) than at fuel-lean conditions (higher EC/TC mass fraction). CAP3070 showed again
225 the opposite behaviour. It is also worth mentioning that for the HePAC and DX280 instruments the measured CE
226 values scattered more at particle sizes larger than 90 nm. This supports the choice of soot with 50-90 nm mobility
227 diameter for the PN-PTI instruments verification linearity tests. The counting efficiency of the different PN-PTI
228 counters as a function of time is shown in Figs. S6-S9 for a measurement duration of 2 min.



229

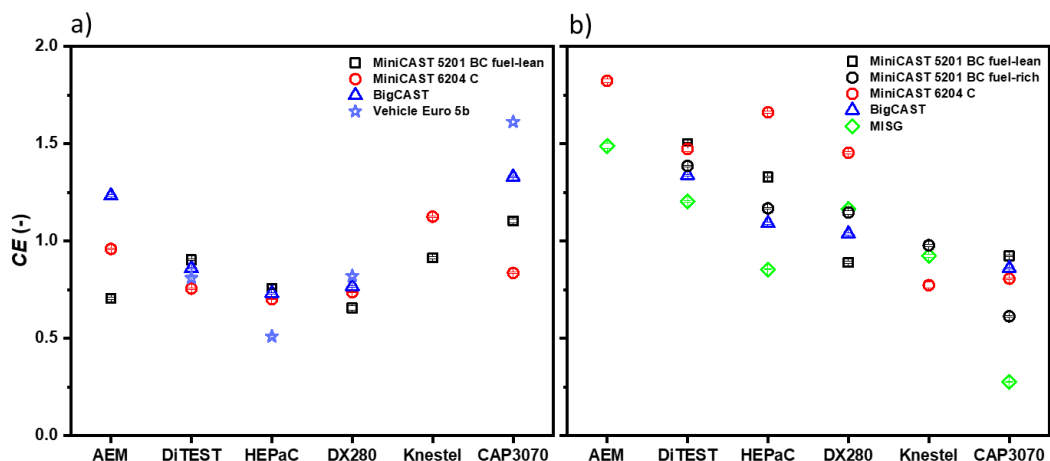


230

231 **Figure 3: Influence of the type of soot generator/vehicle engine (bigCAST, miniCAST 5201 BC, miniCAST 6204 C,**
 232 **MISG and Euro 5b diesel engine) on the counting efficiency (CE) of six different PN-PTI counters: AEM, HEPaC,**
 233 **DiTEST, CAP3070, DX280, and Knestel. The grey-shaded area designates the upper and lower limits in the counting**
 234 **efficiency as defined in the document "Commission Recommendation on particle number measurement for the periodic**
 235 **technical inspection of vehicles equipped with compression ignition engines" (EU, 2023).**

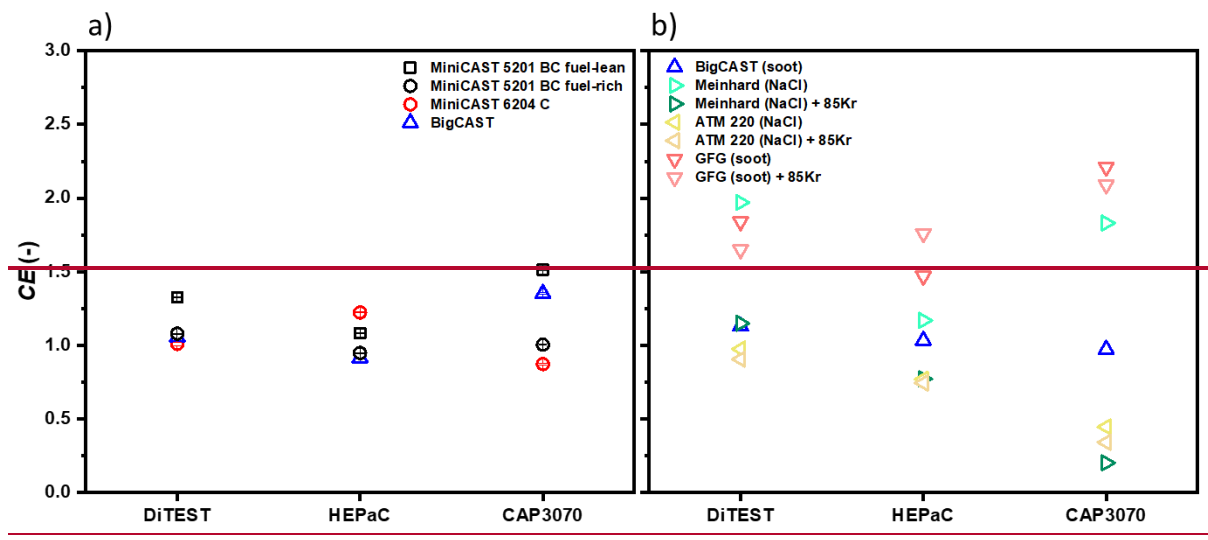
236 In the case of the DX280 and DiTEST, the CEs reported for the laboratory-generated soot (GMD_{mob} of about 50-
 237 55 nm) showed an excellent agreement with the CE measured for diesel soot from a Euro 5b vehicle as shown in
 238 Fig. 4a. In all other cases, deviations were observed. These remained typically within 0.25 units in CE but in one
 239 case (for CAP3070) reached a factor of 2. Note that for real vehicle exhaust the tolerance (maximum permissible
 240 error MPE) according to German regulations is $\pm 50\%$ (PTB, 2021). In general, the data indicate that soot produced

241 by miniCAST and bigCAST generators simulate, in most cases, the properties of diesel soot by a Euro 5b vehicle
 242 satisfactorily.

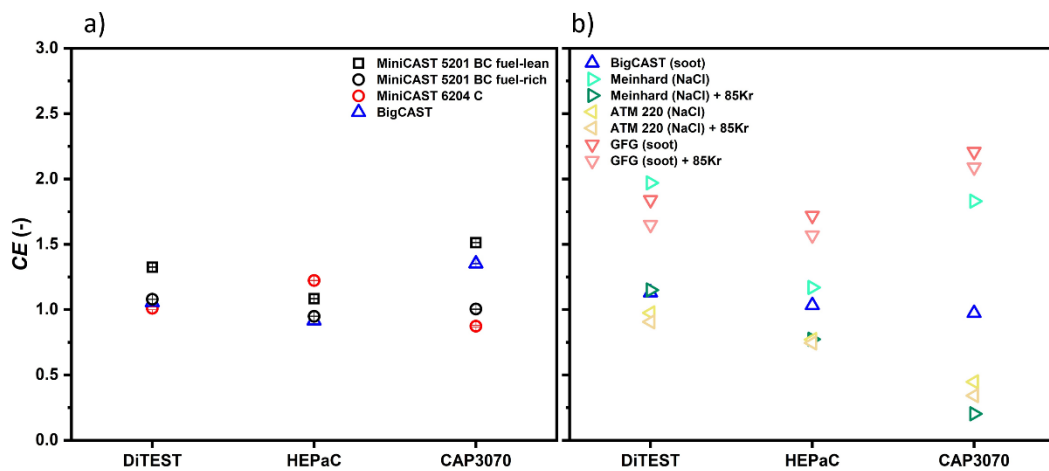


243
 244 **Figure 4: Influence of the type of soot generator/engine (bigCAST, miniCAST 5201 BC, miniCAST 6204 C, MISG, Euro**
 245 **5b vehicle) on the counting efficiencies (CE) of six different PN-PTI counters: AEM, HEPaC, DiTEST, CAP3070,**
 246 **DX280, Knestel (the Knestel and AEM counters were not challenged with the Euro 5b vehicle since the Knestel counter**
 247 **was sent for service and the performance of the AEM counter deteriorated during the measurement campaign at JRC).**
 248 **The polydisperse test aerosols had a particle number concentration of $\sim 100'000 \text{ cm}^{-3}$ and a GMD_{mob} of a) 50-55 nm and**
 249 **b) $\sim 100 \text{ nm}$.**

250 As shown in Fig 4b, soot generated by the MISG ($\text{GMD}_{\text{mob}} \sim 100 \text{ nm}$) led to CEs close to 1 for the DX280,
 251 DiTEST, Knestel and HEPaC counters, and the CEs lied within the tolerance range defined in Germany and
 252 Switzerland (the Netherlands and Belgium only specify a tolerance range for mobility diameters up to 80 nm). The
 253 CE limit values were only exceeded in the case of the AEM and CAP3070 counters but this was most probably
 254 due to a deterioration of the performance of the AEM instrument or an underestimated internal correction and an
 255 overestimated internal correction factor in the case of CAP3070. Although the size of the soot generated by the
 256 MISG ($\text{GMD}_{\text{mob}} \geq 90 \text{ nm}$) tends to be larger than real soot from diesel engines (Kazemimanesh et al., 2019;
 257 Moallemi et al., 2019; Senaratne et al., 2023), it's ease of operation combined with the affordable price make it an
 258 attractive choice for PN-PTI verification in the laboratory.



259



260

261

262 **Figure 5:** a) Influence of different soot aerosols with a GMD_{mob} of ~ 80 nm on the counting efficiencies (CE) of three
 263 different PN-PTI counters. b) Influence of different test aerosols (soot, NaCl and carbonaceous particles from a spark-
 264 discharge generator) on the counting efficiencies (CE) of the same PN-PTI counters. The test aerosols had a GMD_{mob}
 265 of ~ 80 nm. The data points are taken from (Vasilatou et al., 2023).

266 The variation in the counting efficiency of the PN-PTI instruments when tested with soot particles from different
 267 combustion generators (Fig. 5a) is much smaller than that observed with test aerosols such as NaCl or particles
 268 from a spark-discharge generator with a similar GMD_{mob} (Fig. 5b) (Vasilatou et al., 2023). For instance,
 269 carbonaceous particles from a GFG spark-discharge generator (Palas GmbH, Germany) led to a CE of ≥ 2 in the
 270 case of CAP3070 and 1.7-1.8 in the case of DiTEST. On the contrary, CE remained typically in the range 0.7-1.3
 271 when soot was used as test aerosol, irrespective of the type of combustion generator (Fig. 5a). Further studies with
 272 more diesel test vehicles would be necessary to elucidate which type of laboratory-generated soot is the best proxy
 273 for diesel soot, keeping in mind that the properties of real diesel soot can also differ considerably, depending on
 274 the engine design, driving cycle and fuel properties (Hays et al., 2017; Wihersaari et al., 2020).

275 **4 Recommendations**

276 Based on the results of this [and previous studies](#) (Vasilatou et al., 2023), the following recommendations can be
277 made:

- 278 1) Initial and follow-up verification of DC-based PN-PTI counters should ideally be performed with soot as test
279 aerosol. If possible, the same type of combustion generator should be used for the determination of CE during
280 type-examination and verification.
- 281 2) Low-cost soot generators can be a stable source of combustion particles and can be employed for PN-PTI
282 verification using the appropriate setup correction factors. However, the GMD they produce should be in the
283 range 70 ± 20 nm in order to comply with the current linearity verification requirements in Europe.
- 284 3) Laboratory procedures for PN-PTI type-examination and verification should be further harmonised in Europe
285 to avoid inconsistencies in the enforcement of PTI legislation. International round robin tests should be
286 performed to examine whether a) the various PN-PTI instruments type-examined and verified in different
287 European countries according to national regulations exhibit a similar performance and b) whether PN-PTI
288 instruments verified in the same country but with different test aerosols identify defect DPFs in a consistent
289 manner.

290 As highlighted in our previous study (Vasilatou et al., 2023), “setup correction factors” should be determined
291 whenever verification is performed with particles other than soot to account for the effects of the test aerosol on
292 the instrument's counting efficiency. These “setup correction factors” depend on both the aerosol physicochemical
293 properties and the instrument's design, and need to be determined at the NMI level at regular intervals as drifts in
294 the performance of the aerosol generator may occur. If “setup correction factors” are not applied or are inaccurate,
295 the reliability of PTI will be compromised. The use of “setup correction factors” is more critical when nebulisers
296 or spark-discharge generators are used, but special care should also be given to different flame soot generators.
297 This calls for a closer collaboration between NMIs, state authorities, instrument manufacturers and verification
298 centres to ensure fair implementation of regulations in Europe. Further harmonisation of the different PN-PTI
299 type-examination procedures in Europe, e.g. in terms of the combustion generator, would be a valuable first step
300 in order to determine meaningful correction factors for other test aerosols.

301 **5 Conclusions**

302 The type of soot aerosol [generated by diffusion and premixed flame generators](#) affected the response of six
303 different DC-based PN-PTI counters tested in this study. Size and physicochemical properties of the test aerosol
304 had effects on the CE of all counters, [but the effect was different for each counter](#). In most cases, the different
305 laboratory-generated soot aerosols resulted in deviations of 0.25 units in the counting efficiency of individual
306 counters compared to Euro 5b diesel soot at similar mobility diameters (~50-60 nm). It is not entirely clear which
307 type of laboratory-generated soot is the best proxy for real soot emitted by diesel vehicles as the response of the
308 PN-PTI instruments to the different test aerosols was not uniform. It must also be kept in mind that the properties
309 of diesel soot may vary depending on the engine specification and operation. Nevertheless, [the differences](#)
310 [observed with different soot generators were much lower compared to previous studies that used NaCl and particles](#)
311 [from spark discharge generators](#). This study confirms that soot aerosols, irrespective of the generator model, are
312 more suitable as test aerosols [for the PN-PTI application, but special attention should be given to differences that](#)

313 [arise from different generator models or set points and consequently for their correction via appropriately defined](#)
314 [factors than NaCl, oil or particles from spark discharge generators.](#) In view of these results, recommendations were
315 made with regard to PN-PTI type-examination and verification.

316 **Author contribution**

317 All authors designed the experiments. TH, DR and AM carried out the measurement campaigns. TH analysed the
318 data with support from DR. KV prepared the manuscript with contributions from all co-authors.

319 **Competing interests**

320 The authors declare no competing interests.

321 **Acknowledgements**

322 TH, DR, and KV would like to thank Kevin Auderset and Christian Wälchli (both at METAS) for technical support
323 and useful discussions. AM and BG would like to thank Dominique Lesueur and Andrea Bonamin for technical
324 support.

325 **Funding**

326 No external funding was used for this study.

327 **References**

- 328 Anon: Proposal Particulate Number Counters, [online] Available from: [https://nmi.nl/special-particle-number-](https://nmi.nl/special-particle-number-counters/)
329 [counters/](https://nmi.nl/special-particle-number-counters/), n.d.
- 330 AU-Richtlinie: Richtlinie für die Durchführung der Untersuchung der Abgase von Kraftfahrzeugen nach Nummer
331 4.8.2 der Anlage VIIIa StVZO und für die Durchführung von Abgasuntersuchungen an Kraftfahrzeugen nach §
332 47a StVZO (AU-Richtlinie) (Stand 2021), [online] Available from: [https://beck-](https://beck-online.beck.de/Dokument?vpath=bibdata%5Cges%5Cbrd_013_2008_0196%5Ccont%5Cbrd_013_2008_0196.htm)
333 [online.beck.de/Dokument?vpath=bibdata%5Cges%5Cbrd_013_2008_0196%5Ccont%5Cbrd_013_2008_0196.ht](https://beck-online.beck.de/Dokument?vpath=bibdata%5Cges%5Cbrd_013_2008_0196%5Ccont%5Cbrd_013_2008_0196.htm)
334 [m](https://beck-online.beck.de/Dokument?vpath=bibdata%5Cges%5Cbrd_013_2008_0196%5Ccont%5Cbrd_013_2008_0196.htm), n.d.
- 335 Bischof, O. F., Weber, P., Bundke, U., Petzold, A. and Kiendler-Scharr, A.: Characterization of the Miniaturized
336 Inverted Flame Burner as a Combustion Source to Generate a Nanoparticle Calibration Aerosol, *Emiss. Control*
337 *Sci. Technol.*, 6(1), 37–46, doi:10.1007/S40825-019-00147-W/METRICS, 2020.
- 338 Botero, M. L., Londoño, J., Agudelo, A. F. and Agudelo, J. R.: Particle Number Emission for Periodic Technical
339 Inspection in a Bus Rapid Transit System, *Emiss. Control Sci. Technol.*, 9, 128–139, doi:10.2139/ssrn.4246867,
340 2023.
- 341 Burtscher, H., Lutz, T. and Mayer, A.: A New Periodic Technical Inspection for Particle Emissions of Vehicles,
342 *Emiss. Control Sci. Technol.* 2019 53, 5(3), 279–287, doi:10.1007/S40825-019-00128-Z, 2019.
- 343 Dhaniyala, S., Fierz, M., Keskinen, J. and Marjamäki, M.: Instruments Based on Electrical Detection of Aerosols
344 Aerosol Measurement, in *Aerosol Measurement: Principles, Techniques, and Applications*, edited by P. Kulkarni,
345 P. A. Baron, and K. Willeke, pp. 393–416, John Wiley & Sons, Inc., Hoboken, New Jersey., 2011.
- 346 Ess, M. N. and Vasilatou, K.: Characterization of a new miniCAST with diffusion flame and premixed flame

347 options: Generation of particles with high EC content in the size range 30 nm to 200 nm, *Aerosol Sci. Technol.*,
348 53(1), 29–44, doi:10.1080/02786826.2018.1536818, 2019.

349 Ess, M. N., Bertò, M., Keller, A., Gysel-Beer, M. and Vasilatou, K.: Coated soot particles with tunable, well-
350 controlled properties generated in the laboratory with a miniCAST BC and a micro smog chamber, *J. Aerosol Sci.*,
351 157, 105820, doi:10.1016/j.jaerosci.2021.105820, 2021a.

352 Ess, M. N., Bertò, M., Irwin, M., Modini, R. L., Gysel-Beer, M. and Vasilatou, K.: Optical and morphological
353 properties of soot particles generated by the miniCAST 5201 BC generator, *Aerosol Sci. Technol.*, 55(7), 828–
354 847, doi:10.1080/02786826.2021.1901847, 2021b.

355 EU: COMMISSION RECOMMENDATION (EU) 2023/688 of 20 March 2023 on particle number measurement
356 for the periodic technical inspection of vehicles equipped with compression ignition engines, *Off. J. Eur. Union*,
357 (715), 46–64 [online] Available from: [https://eur-lex.europa.eu/legal-](https://eur-lex.europa.eu/legal-content/EN/TXT/?uri=CELEX%3A32023H0688)
358 [content/EN/TXT/?uri=CELEX%3A32023H0688](https://eur-lex.europa.eu/legal-content/EN/TXT/?uri=CELEX%3A32023H0688), 2023.

359 Fierz, M., Houle, C., Steigmeier, P. and Burtscher, H.: Design, calibration, and field performance of a miniature
360 diffusion size classifier, *Aerosol Sci. Technol.*, 45(1), 1–10, doi:10.1080/02786826.2010.516283, 2011.

361 Filippov, A. V., Zurita, M. and Rosner, D. E.: Fractal-like aggregates: Relation between morphology and physical
362 properties, *J. Colloid Interface Sci.*, 229(1), 261–273, doi:10.1006/jcis.2000.7027, 2000.

363 Frank, Adam, Olfert, J., Wong, K.-F., Kunert, S. and Richter, J. M.: Effect of Engine-Out Soot Emissions and the
364 Frequency of Regeneration on Gasoline Particulate Filter Efficiency, *SAE Tech. Pap.*, 2020-01-14,
365 doi:10.4271/2020-01-1431, 2020.

366 Giechaskiel, B. and Melas, A.: Comparison of Particle Sizers and Counters with Soot-like, Salt, and Silver
367 Particles, *Atmosphere (Basel)*, 13(10), doi:10.3390/atmos13101675, 2022.

368 Giechaskiel, B., Ntziachristos, L. and Samaras, Z.: Effect of ejector dilutors on measurements of automotive
369 exhaust gas aerosol size distributions, *Meas. Sci.*, 20, 045703, doi:10.1088/0957-0233/20/4/045703, 2009.

370 Giechaskiel, B., Forloni, F., Carriero, M., Baldini, G., Castellano, P., Vermeulen, R., Kontses, D., Fragkiadoulakis,
371 P., Samaras, Z. and Fontaras, G.: Effect of Tampering on On-Road and Off-Road Diesel Vehicle Emissions,
372 *Sustainability*, 14(10), 6065, doi:10.3390/su14106065, 2022.

373 Hays, M. D., Preston, W., George, B. J., George, I. J., Snow, R., Faircloth, J., Long, T., Baldauf, R. W. and
374 McDonald, J.: Temperature and Driving Cycle Significantly Affect Carbonaceous Gas and Particle Matter
375 Emissions from Diesel Trucks, *Energy and Fuels*, 31(10), 11034–11042, doi:10.1021/acs.energyfuels.7b01446,
376 2017.

377 Kazemimanesh, M., Moallemi, A., Thomson, K., Smallwood, G., Lobo, P. and Olfert, J. S.: A novel miniature
378 inverted-flame burner for the generation of soot nanoparticles, *Aerosol Sci. Technol.*, 53(2), 184–195,
379 doi:10.1080/02786826.2018.1556774, 2019.

380 Kesselmeier, J. and Staudt, M.: An Overview on Emission, Physiology and Ecology, *J. Atmos. Chem.*, 33, 23–88
381 [online] Available from: [https://link-springer-](https://link.springer-com.ez27.periodicos.capes.gov.br/content/pdf/10.1023%2FA%3A1006127516791.pdf)
382 [com.ez27.periodicos.capes.gov.br/content/pdf/10.1023%2FA%3A1006127516791.pdf](https://link.springer-com.ez27.periodicos.capes.gov.br/content/pdf/10.1023%2FA%3A1006127516791.pdf), 1999.

383 Kheirbek, I., Haney, J., Douglas, S., Ito, K. and Matte, T.: The contribution of motor vehicle emissions to ambient
384 fine particulate matter public health impacts in New York City: A health burden assessment, *Environ. Heal. A*
385 *Glob. Access Sci. Source*, 15(1), doi:10.1186/s12940-016-0172-6, 2016.

386 Kurniawan, A. and Schmidt-Ott, A.: Monitoring the soot emissions of passing cars, *Environ. Sci. Technol.*, 40(6),
387 1911–1915, doi:10.1021/es051140h, 2006.

388 Lehtimäki, M.: Modified Electrical Aerosol Detector, in *Aerosols in the Mining and Industrial Work*
389 *Environments: Instrumentation* (Vol. 3), edited by B. Y. H. Liu and V. A. Marple, pp. 1135–1143, Ann Arbor
390 Science Publishers., 1983.

391 Ligterink, N. E.: *Diesel Particle Filters.*, 2018.

392 Mandelbrot, B. B.: *The fractal geometry of nature*, Freeman, W. H., San Francisco., 1982.

393 Melas, A., Selleri, T., Suarez-Bertoa, R. and Giechaskiel, B.: Evaluation of solid particle number sensors for
394 periodic technical inspection of passenger cars, *Sensors*, 21(24), 8325, doi:10.3390/s21248325, 2021.

395 Melas, A., Selleri, T., Suarez-Bertoa, R. and Giechaskiel, B.: Evaluation of Measurement Procedures for Solid
396 Particle Number (SPN) Measurements during the Periodic Technical Inspection (PTI) of Vehicles, *Int. J. Environ.*
397 *Res. Public Health*, 19(13), 7602, doi:10.3390/ijerph19137602, 2022.

398 Melas, A., Vasilatou, K., Suarez-Bertoa, R. and Giechaskiel, B.: Laboratory measurements with solid particle
399 number instruments designed for periodic technical inspection (PTI) of vehicles, *Measurement*, 215(April),
400 112839, doi:10.1016/j.measurement.2023.112839, 2023.

401 Melas, A. D., Isella, L., Konstandopoulos, A. G. and Drossinos, Y.: Friction coefficient and mobility radius of
402 fractal-like aggregates in the transition regime, *Aerosol Sci. Technol.*, 48(12), 1320–1331,
403 doi:10.1080/02786826.2014.985781, 2014.

404 Moallemi, A., Kazemimanesh, M., Corbin, J. C., Thomson, K., Smallwood, G., Olfert, J. S. and Lobo, P.:
405 Characterization of black carbon particles generated by a propane-fueled miniature inverted soot generator, *J.*
406 *Aerosol Sci.*, 135, 46–57, doi:10.1016/J.JAEROSCI.2019.05.004, 2019.

407 Olfert, J. and Rogak, S.: Universal relations between soot effective density and primary particle size for common
408 combustion sources, *Aerosol Sci. Technol.*, 53(5), 485–492, doi:10.1080/02786826.2019.1577949, 2019.

409 Pang, Y., Wang, Y., Wang, Z., Zhang, Y., Liu, L., Kong, S., Liu, F., Shi, Z. and Li, W.: Quantifying the Fractal
410 Dimension and Morphology of Individual Atmospheric Soot Aggregates, *J. Geophys. Res. Atmos.*, 127(5),
411 e2021JD036055, doi:10.1029/2021JD036055, 2022.

412 Pang, Y., Chen, M., Wang, Y., Chen, X., Teng, X., Kong, S., Zheng, Z. and Li, W.: Morphology and Fractal
413 Dimension of Size-Resolved Soot Particles Emitted From Combustion Sources, *J. Geophys. Res. Atmos.*, 128(6),
414 e2022JD037711, doi:10.1029/2022JD037711, 2023.

415 PTB: PTB-Anforderungen 12.16 „Partikelzähler“ (05/2021), [online] Available from:
416 <https://doi.org/10.7795/510.20210623>, 2021.

417 Senaratne, A., Olfert, J., Smallwood, G., Liu, F., Lobo, P. and Corbin, J. C.: Size and light absorption of miniature-
418 inverted-soot-generator particles during operation with various fuel mixtures, *J. Aerosol Sci.*, 170(February),
419 106144, doi:10.1016/j.jaerosci.2023.106144, 2023.

420 Sorensen, C. M.: The mobility of fractal aggregates: A review, *Aerosol Sci. Technol.*, 45(7), 765–779,
421 doi:10.1080/02786826.2011.560909, 2011.

422 Tavakoli, F. and Olfert, J. S.: Determination of particle mass, effective density, mass-mobility exponent, and
423 dynamic shape factor using an aerodynamic aerosol classifier and a differential mobility analyzer in tandem, *J.*
424 *Aerosol Sci.*, 75, 35–42, doi:10.1016/j.jaerosci.2014.04.010, 2014.

425 US-EPA: *Integrated Science Assessment for Particulate Matter.* [online] Available from:
426 <https://www.epa.gov/isa/integrated-science-assessment-isa-particulate-matter>, 2019.

427 UVEK: *Verordnung des UVEK über Wartung und Nachkontrolle von Motorwagen betreffend Abgas- und*
428 *Rauchemissionen (SR 741.437),*, 1–18 [online] Available from: <https://www.fedlex.admin.ch/eli/cc/2002/596/de>,

429 2023.
430 VAMV: Verordnung des EJPD über Abgasmessmittel für Verbrennungsmotoren (VAMV), [online] Available
431 from: <https://www.fedlex.admin.ch/eli/cc/2006/251/de>, 2018.
432 Vasilatou, K., Kok, P., Pratzler, S., Nowak, A., Waheed, A., Buekenhoudt, P., Auderset, K. and Andres, H.: New
433 periodic technical inspection of diesel engines based on particle number concentration measurements, OIML Bull.,
434 LXIII, 11–16 [online] Available from:
435 https://www.oiml.org/en/publications/bulletin/pdf/oiml_bulletin_july_2022.pdf, 2022.
436 Vasilatou, K., Wälchli, C., Auderset, K., Burtscher, H., Hammer, T., Giechaskiel, B. and Melas, A.: Effects of the
437 test aerosol on the performance of periodic technical inspection particle counters, *J. Aerosol Sci.*, 172(January),
438 doi:10.1016/j.jaerosci.2023.106182, 2023.
439 Wang, Y., Liu, F., He, C., Bi, L., Cheng, T., Wang, Z., Zhang, H., Zhang, X., Shi, Z. and Li, W.: Fractal
440 Dimensions and Mixing Structures of Soot Particles during Atmospheric Processing, *Environ. Sci. Technol. Lett.*,
441 4(September 2019), 487–493, doi:10.1021/acs.estlett.7b00418, 2017.
442 WHO: WHO global air quality guidelines, *Coast. Estuar. Process.*, 1–360 [online] Available from:
443 <https://apps.who.int/iris/handle/10665/345329>, 2021.
444 Wihersaari, H., Pirjola, L., Karjalainen, P., Saukko, E., Kuuluvainen, H., Kulmala, K., Keskinen, J. and Rönkkö,
445 T.: Particulate emissions of a modern diesel passenger car under laboratory and real-world transient driving
446 conditions, *Environ. Pollut.*, 265, doi:10.1016/j.envpol.2020.114948, 2020.
447
448

